Experimental Strain Response-Envelopes of Granular Materials for Monotonous and Low-Cycle Loading Processes

S. Danne and A. Hettler

Abstract To look onto the stress-path-dependent strain behaviour of granular soils at low-cycle and monotonous loading processes as a basis for the development of new, improved or enhanced constitutive models, drained, stress-controlled triaxial-tests with a fine grained sand have been carried out. The focus was to investigate total as well as quasi-elastic strains for different stress-states by means of strain-response-envelopes. By subtracting the quasi-elastic strains from the total strains, a separate evaluation of plastic strains was also possible. For monotonous loading one separate soil-specimen has been used for each monotonous loading-direction. The shapes of the response-envelopes for initially isotropic stress-states were similar to ellipses, for initially anisotropic stress-states their shape was elongated and shifted away in the direction of the failure lines. For low-cycle loading, cycles of relatively small stress increments were applied in different directions in the stress-plane. It is found that quasi-elastic behaviour can already occur at a low number of cycles. The shapes of the obtained strain-response-envelopes were similar to symmetrical ellipses. It could be observed that the size of the ellipses decreases with increasing mean pressure p. The major axis of the ellipses rotates depending on the initial stress-state $\eta = q/p$, indicating a stress-induced anisotropy. Preloading seems to have little effect on the stiffness or the directions of the quasi-elastic strains. In the future it is intended to simulate the observed stress-strain behaviour by means of new, improved or enhanced constitutive models.

Keywords Triaxial tests · Strain response-envelopes · Incremental stress-strain behaviour · Granular soils

S. Danne (✉) · A. Hettler
Chair of Soil Mechanics and Foundation Engineering, Technical University of Dortmund, Dortmund, Germany
e-mail: stefanie.danne@tu-dortmund.de

Th. Triantafyllidis (ed.), *Holistic Simulation of Geotechnical Installation Processes*,
Lecture Notes in Applied and Computational Mechanics 77,
DOI 10.1007/978-3-319-18170-7_12

1 Introduction

Due to quasi-static loading with cyclic progression there are plastic, i.e. irreversible, and elastic, i.e. reversible, deformations in the soil, without reaching fully elastic behaviour. In the quasi-elastic regime the material behaves asymptotically elastic. Goldscheider [10] describes this behaviour as "material shakedown".

Considering the number of cycles one can distinguish between high-cycle and low-cycle loading processes.

Effects of wind load on foundations of wind energy plants, vehicle crossing on foundation constructions, vibrating of foundation-elements e.g. retaining-wall-elements or grouted piles can be related to high-cycle loading. The number of cycles N during these processes is very high ($N \gg 50$). Due to accumulation of numerical errors and high computing time an implicit calculation of displacements, where the deformations during one cycle are calculated separately and accumulated, is not adequate. Instead, deformations due to high-cycle loading are calculated by using explicit models. Here the calculation of irreversible strains can be treated similar to creep deformations under constant loads, Niemunis et al. [20].

Low cycle loading processes can be defined for a lower number of cycles with ($N \leq 50$), see Danne and Hettler [6]. Deformations in this case are usually calculated implicitly, i.e. separately for each cycle and then accumulated.

Subject of this paper are low-cycle loading processes, of which it is assumed that inertial forces are negligible [12]. Un- and reloading for example, occurring during the construction phase of multiple braced excavation walls, produce stress paths quite similar to those of cyclically loaded systems at the first cycles before reaching shakedown. Therefore, these processes are also included within the scope of low-cycle loading.

An external cyclic load on a foundation for example does not lead to cyclic behaviour right from the beginning. This is the case only after a certain number of cycles. Some examples for low-cycle loading processes and related un- and reloading processes are:

- construction stages of multiple braced or anchored excavation walls
- braced excavation with force-controlled struts (to control deformations)
- temperature exposure of struts
- filling and emptying of locks or silos during first utilisation phase
- summer-/winter position of abutments of integral bridges due to temperature differences

The simplified consideration of a soil element behind a strutted retaining wall for example shows, that monotonous stress-paths as well as repeated low-cycle loading process with various directions can occur, Fig. 1.

In front of the embedded part of the wall stress-paths are similar, but extension may be important instead of compression.

Figure 2 shows typical stress-paths of a soil element beneath a watergate's bottom during construction and first utilisation phase of the lock. Stress-states in extension may appear here, too.

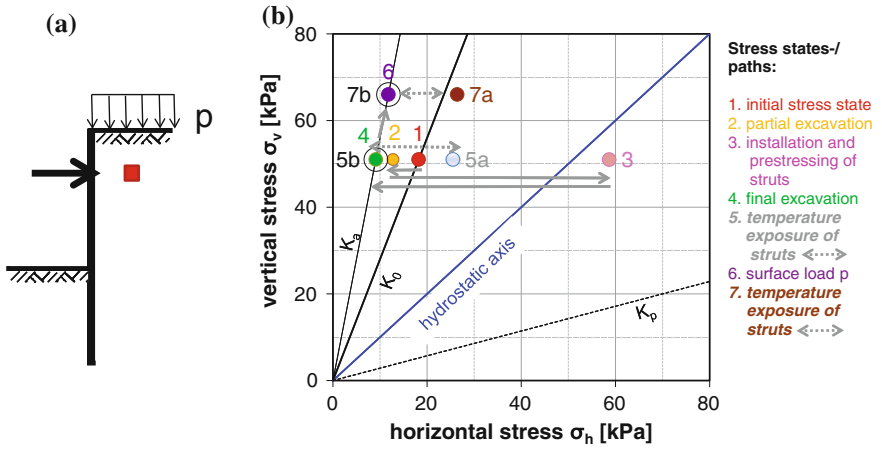

Fig. 1 Typical stress-paths (**b**) in a soil-element behind an excavation-wall (**a**)

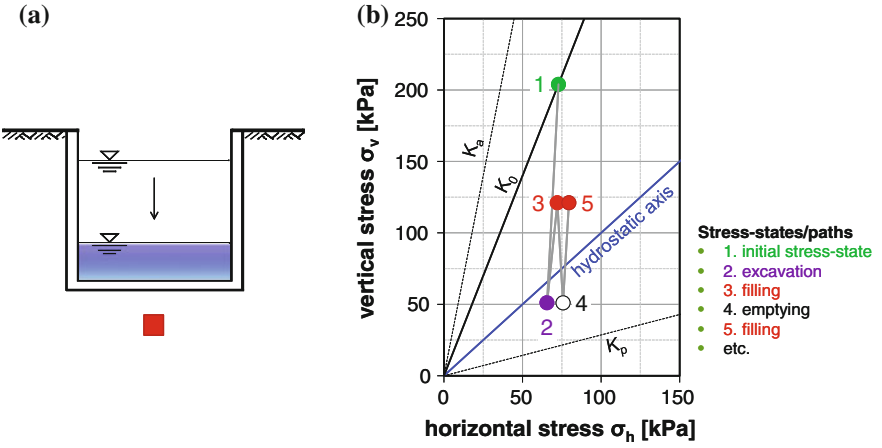

Fig. 2 Possible stress-paths during construction and first utilisation phase of a watergate (**b**) in a soil element beneath a watergate's bottom (**a**)

Element tests investigating the stress-strain behaviour of soils must therefore take into account any stress-path and monotonous as well as repeated un- and reloading processes when contributing successfully to the development of new or enhanced constitutive equations. It is also obvious, that stress-states in compression as well as in extension have to be considered.

2 Response-Envelopes

2.1 *Stress- and Strain-Components in Triaxial Testing*

Figure 3 shows the axisymmetric stress- and strain-components referred to in this paper.

In axial symmetric conditions $\sqcup_1$ denotes the axial component and $\sqcup_3$ the lateral component of stress or strain respectively.

The Roscoe invariants, mean pressure p and the deviatoric stress q, are defined as:

$$p = (\sigma_1 + 2\sigma_3)/3, \tag{1}$$

$$q = \sigma_1 - \sigma_3. \tag{2}$$

2 vectors, which are orthogonal to each other in the 3-dimensional principal stress space σ_1-σ_2-σ_3, are not perpendicular to each other anymore in the p-q-plane and their lengths get distorted. To avoid this, stresses and strains in this paper are presented in the rendulic plane, which is isomorphic. Its horizontal axis is $\sqrt{2}\sigma_3$ and $\sqrt{2}\varepsilon_3$ respectively and the vertical axis σ_1 and ε_1 (Fig. 4). The stress-ratio

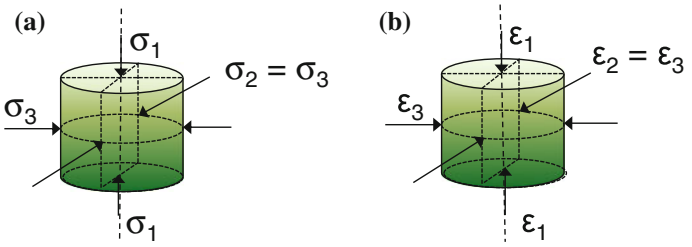

Fig. 3 Stress-(**a**) and strain (**b**)-components in triaxial testing

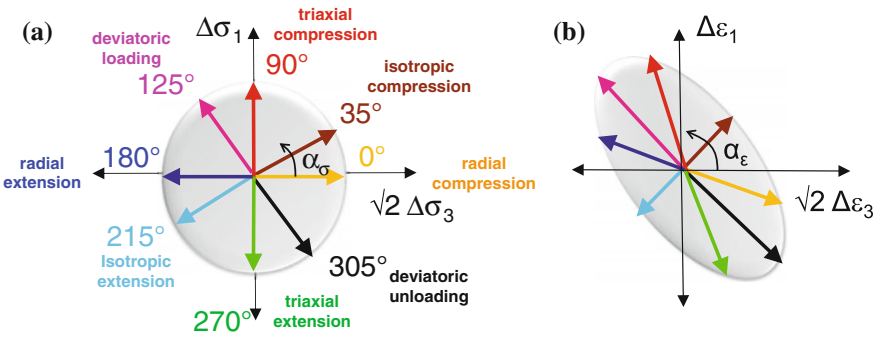

Fig. 4 Applied stress $\Delta\sigma$ increments (**a**) and corresponding strain responses (**b**) for different directions α_σ

$$\eta = q/p \tag{3}$$

describes the stress-state's position in the p-q-plane.

For all tests described in this paper were carried out drained, all stresses referred to are effective stresses ($\sigma = \sigma'$).

2.2 Concept

New or improved constitutive models need to be validated and calibrated. This is often done with the aid of experimental as well as numerical element tests, for example triaxial or oedometer tests. So called response-envelopes are a useful tool for calibrating, validating and comparing constitutive equations [1, 7, 15, 22, 23].

First basics of response-envelopes were presented in the 1970s by Lewin and Burland [17]. A few years later Gudehus [11] used this concept in context with the development of constitutive equations.

To obtain a response-envelope, a soil element is subjected to a certain stress- or strain-increment. The corresponding "response" of the soil in terms of either strain or stress is determined and presented graphically. The direction of the implied stress or strain increment with a constant absolute value is varied and leads to different stress or strain responses, endpoints of which are connected to a response-envelope. Considering the concept of strain-response-envelopes dealt with in this paper, a constant stress increment

$$\Delta\sigma = \sqrt{\Delta\sigma_1^2 + 2\Delta\sigma_3^2} \tag{4}$$

for at least 8 different stress probe directions α_σ is shown in Fig. 4a.

The strains too are plotted in the isomorphic rendulic diagram, where the resulting total strain-increment is

$$\Delta\varepsilon = \sqrt{\Delta\varepsilon_1^2 + 2\Delta\varepsilon_3^2}. \tag{5}$$

The 2 angles, α_σ and α_ε, shown in Fig. 4, are used herein to quantify the direction of incremental quantities where α_σ is the angle between stress probe vector and the positive $\sqrt{2}\sigma_3$-axis, (6), and α_ε is the angle between the strain increment vector and the positive $\sqrt{2}\Delta\varepsilon_3$-axis, (7). The angles are measured counter clockwise [1]

$$\alpha_\sigma = \arctan\frac{\Delta\sigma_1}{\sqrt{2}\Delta\sigma_3} \qquad \text{with } \alpha_\sigma \in [0; 360) \tag{6}$$

$$\alpha_\varepsilon = \arctan\frac{\Delta\varepsilon_1}{\sqrt{2}\Delta\varepsilon_3} \qquad \text{with } \alpha_\varepsilon \in [0; 360). \tag{7}$$

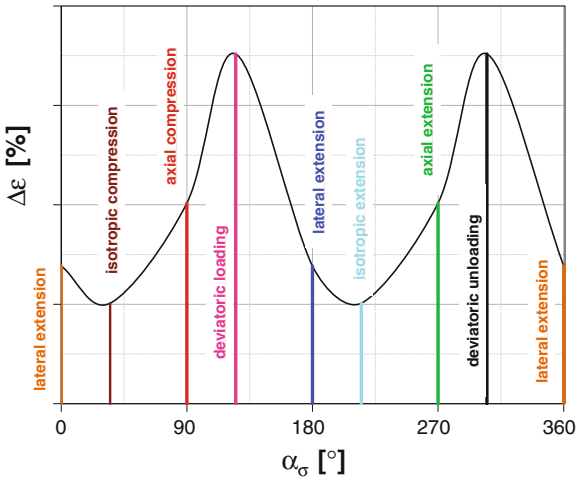

Fig. 5 Absolute value of strain increment $\Delta\varepsilon$ versus stress probe direction α_σ

As $\Delta\sigma$ = const. for all directions α_σ, one gets a circle in isomorphic diagrams, Fig. 4a. The red and the green lines in Fig. 4 for example represent triaxial compression/extension with $\Delta\sigma_3 = 0$. The brown and the turquoise lines stand for isotropic compression/extension with $\Delta q = 0$. A strain response in solely vertical direction ($\Delta\varepsilon_3 = 0$), i.e. a vertical arrow-line in Fig. 4b, would result from a K_0-stress path, which is—for the examined density with Jaky-$K_0 \approx 0.37$—an arrow line inclined under $\alpha_\sigma \approx 62°$ in Fig. 4a.

To show the correlation between the stress probe direction α_σ and the absolute value of the strain increment vector $\Delta\varepsilon$ defined in (5), an alternative evaluation method is to plot the strains $\Delta\varepsilon$ versus the angle of the stress-probe direction α_σ, Fig. 5.

From Fig. 5 it can be seen, which loading directions lead to the largest and smallest absolute strains respectively.

Performing stress-probe-experiments and evaluating the results with the concept of response-envelopes is a convenient tool to investigate the incremental stress-strain behaviour during first loading as well as during un- and reloading-processes.

In this paper the total as well as the quasi-elastic part of the strains due to a relatively low number of un- and reloading-processes ("low-cycle loading") is investigated and evaluated by means of strain-response-envelopes.

2.3 Literature

Some experimental tests to investigate the incremental stress-strain behaviour by means of response-envelopes can be found in literature. On the one hand, there are experiments which focus on either **the total** or **the plastic strains**. On the other

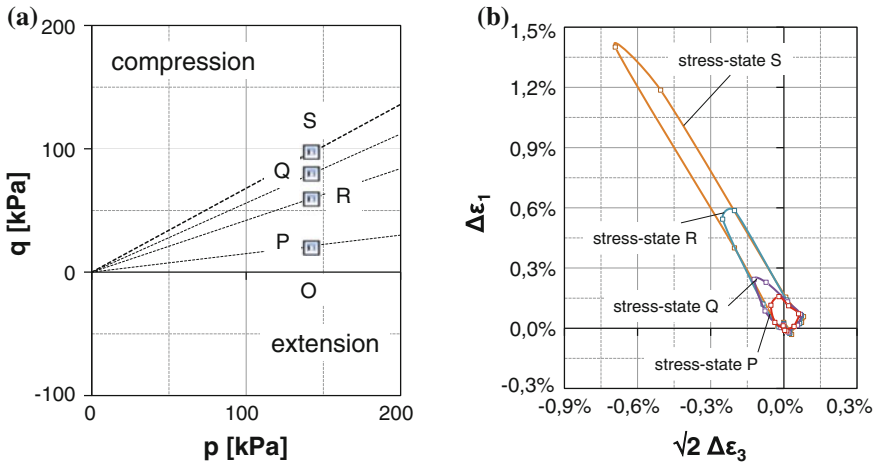

Fig. 6 Initial stress-states (**a**) and strain response-envelopes (**b**) of Lewin and Burland's experiments [17]

hand, there are experiments where very small stress- or strain-cycles are applied in different directions e.g. to investigate the cross-anisotropic **quasi-elastic properties** of the soil.

2.3.1 Stress- or Strain Probe Experiments Investigating Total or Plastic Strains

In the 1970s Lewin and Burland [17] performed stress-controlled triaxial tests on a remoulded, saturated, powdered slate dust. Their tests were performed from 5 initial stress-states shown in Fig. 6a. Lewin and Burland showed that using the normality condition of plasticity theory provides a reasonable basis for the prediction of shear strain behaviour. They found evidence that the direction of the plastic strain increment vector depends on the direction of the stress probe vector $\Delta\sigma$.

Anandarajah et al. [1] performed a series of stress-probe experiments on dense and medium dense Ottawa sand to investigate the dependence of magnitude and direction of incremental plastic strain on direction of incremental stress. 6 different initial stress-states were chosen and stress increments from $\Delta\sigma = 9$–52 kPa in up to 10 different directions were applied on triaxial sand specimens, Fig. 7. The focus was set on plastic strains, which were evaluated by subtracting the elastic strains from the total strains. The elastic strains again were either calculated "by using suitable elastic properties" [1] or determined by applying a stress cycle and measuring the elastic strains during reversal. The results conform to the theory of plasticity for stress-states close to the failure line. It differs from it for stress-states close to the isotropic axis.

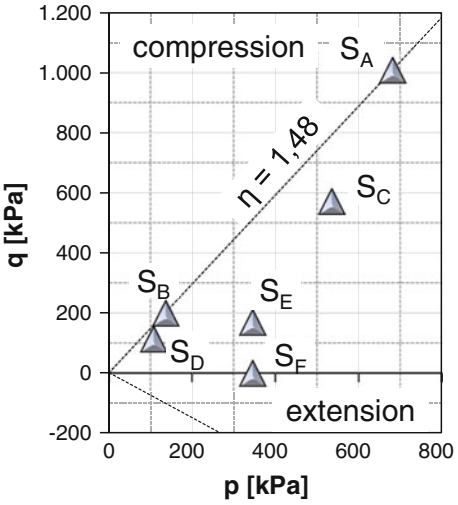

Fig. 7 Initial stress-states of Anandarajah's experiments [1]

Royis and Doanh [21] reported of strain-response-envelopes carried out at 3 initial stress-states for dense Hostun sand, Fig. 8a. The strains due to $\Delta\sigma = 10$ kPa were determined and presented graphically by strain-response-envelopes, Fig. 8b, c. For each stress probe direction, one soil-sample was used, so that the determined strain increments can be interpreted as total strains at first loading. Quasi-elastic strains were not investigated.

Calvetti et al. [4] used Doanh's results for a large numerical study with their Discrete-Element-Model (DEM) and compared the obtained with the experimental results.

Costanzo et al. [5] performed several triaxial tests on a silty clay to obtain strain-response-envelopes at 2 different initial stress-states, Fig. 9a. The strains were investigated and plotted for stress-increments between $\Delta\sigma = 20$ and 90 kPa, Fig. 9b, c (envelope for $\Delta\sigma = 90$ kPa not shown for sake of clarity). They found the response-envelopes to be consistent with each other, indicating an inelastic and irreversible material response, i.e. a strong dependence on the stress increment direction, also at relatively small strain levels. Quasi-elastic strains were not considered explicitly here either.

2.3.2 Stress- or Strain Probe Experiments Investigating Quasi-Elastic Strains

There is hardly any literature where "quasi-elastic" strain-response-envelopes due to low or high-cycle loading are presented. There are some papers though, in which quasi-elastic stress-strain-behaviour is investigated after applying very small axial and radial stress- or strain amplitudes. The object of these experiments is mainly to investigate the soil's inherent and stress-state-induced anisotropy at small

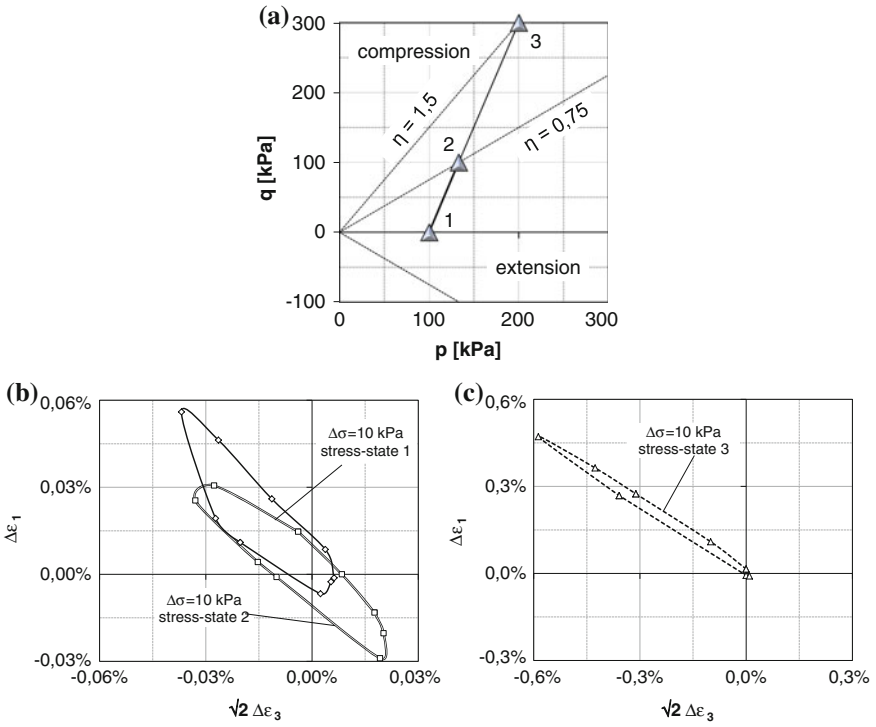

Fig. 8 Initial stress-states (**a**) and response-envelopes (**b**, **c**) of Royis and Doanh's experiments [21]

strain-regime. Hoque and Tatsuoka [14] for example investigated inherent and stress-state-induced anisotropy of different sands. They applied very small strain-amplitude cyclic normal stresses in vertical as well as horizontal direction at different initial isotropic and anisotropic stress-states, see Sect. 5.6 of this paper.

Ezaoui and Di Benedetto [9] carried out experiments to determine the quasi-elastic properties of dry Hostun sand. Very small axial cyclic static loadings and piezoelectric sensor-waves at different levels of the stress-strain curve were applied. The authors also investigated the influence of 3 different sample preparation-methods on anisotropic elastic behaviour, see Sect. 5.6 of this paper.

Kuwano et al. [16] imposed small shear waves to cylindrical sand samples at different stress-states to investigate the effect of stress ratio on anisotropic quasi-elastic properties.

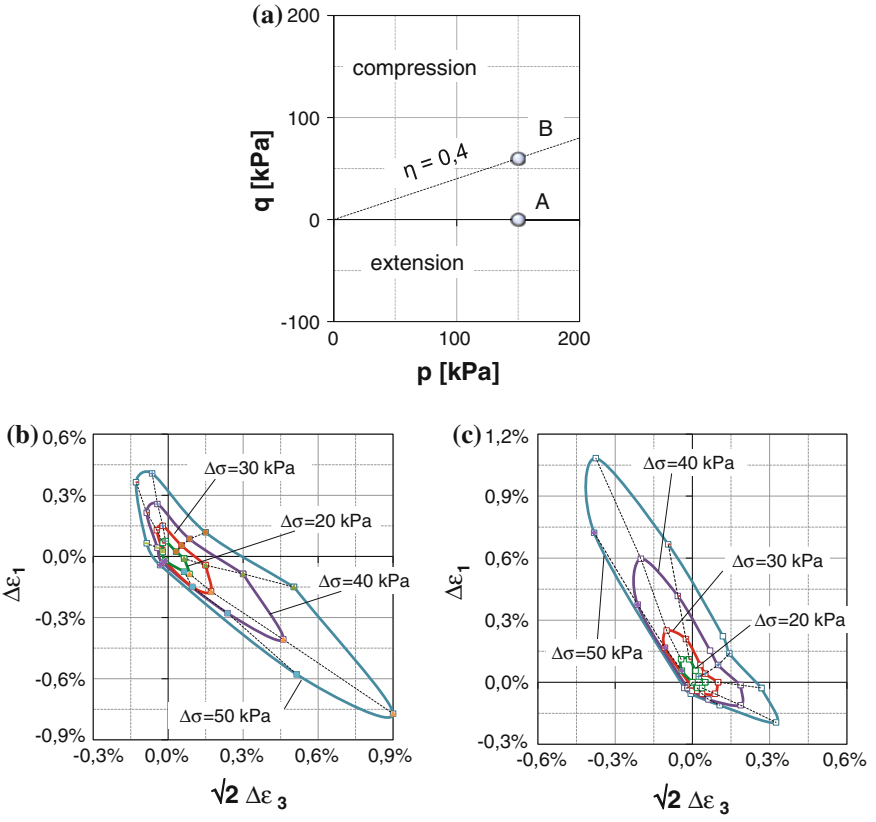

Fig. 9 Initial stress-states (**a**) and corresponding strain-response-envelopes at isotropic stress-state (**b**) and anisotropic stress-state (**c**) of Costanzo's experiments [5]

3 Experimental Fundamentals

3.1 Triaxial Device and Measuring Technique

The triaxial device used for the presented experiments is equipped with high-resolution measurement- and control-technology. It is equipped with an external force transducer to measure the axial strain and a volume-measuring device (burette) with a highly sensitive pressure sensor to measure the volumetric strain. The force transducer enters the cell through a ball bushing linear bearing and the force is measured internally. To avoid tilting, it is connected rigidly to the cell top, Fig. 10.

The confining pressure as well as the axial force can be controlled independently, so that any stress-path from any initial stress-state can be performed, either monotonously or cyclically. Height and diameter of the soil specimen are 10 cm.

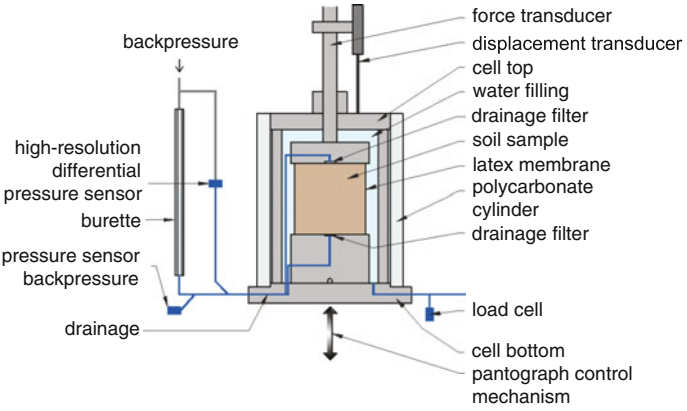

Fig. 10 Triaxial device

Radial strains are determined indirectly from measured axial and volumetric strains. For stress-increments $\Delta\sigma \leq 20 \ldots 50$ kPa, this procedure has led to plausible and reproducible experimental results of sufficient accuracy, Costanzo et al. [5], Anandarajah et al. [1].

To minimise end-friction, the specimen's end plates were first lubricated with a thin layer of silicon grease and then covered with a thin latex membrane ($t_M = 0.35$ mm). This method also contributes to a homogenous distribution of stress within the specimen.

3.2 Tested Sand

As the volumetric strains ε_v are measured via in- and out coming pore water and not only the axial stress σ_1, but also the cell pressure is varied, effects of membrane penetration also have to be taken into account, Nicholson et al. [18] and Baldi and Nova [2]. To minimise possible errors a fine-grained sand with a low uniformity-index C_U was used, Fig. 11.

3.3 Testing Procedure

The soil sample was fabricated by pluviating the dry sand, thereby maintaining a constant initial height. This specimen-preparation-method was kept constant for all tests. The achieved relative densities I_D were well reproducible with little deviation (± 0.1).

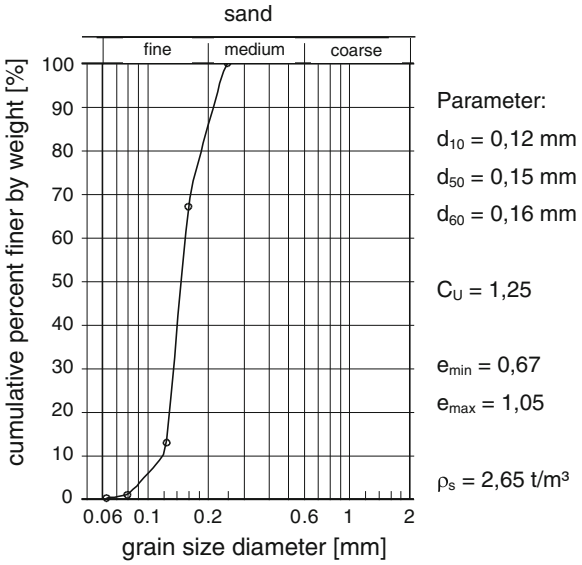

Fig. 11 Grain size distribution curve of the sand

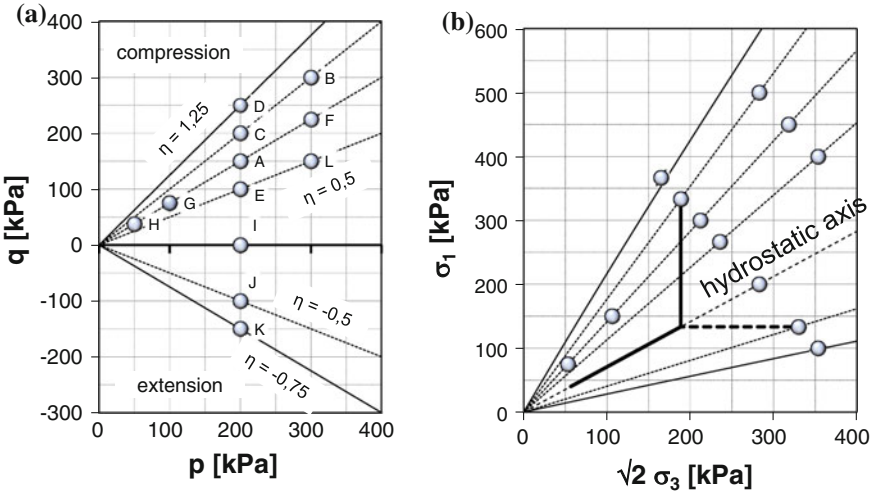

Fig. 12 Investigated stress-states (**a**) and reaching them (**b**)

The soil sample was then flushed with carbon dioxide (CO_2) for about 1 h and saturated with deaired water afterwards. After that a predefined initial stress-state (Fig. 12a) was reached, either by increasing the vertical stress (for stress-states in compression, solid line in Fig. 12b) or the horizontal stress (for stress-states in extension, dashed line in Fig. 12b). The backpressure was kept constant at 200 kPa.

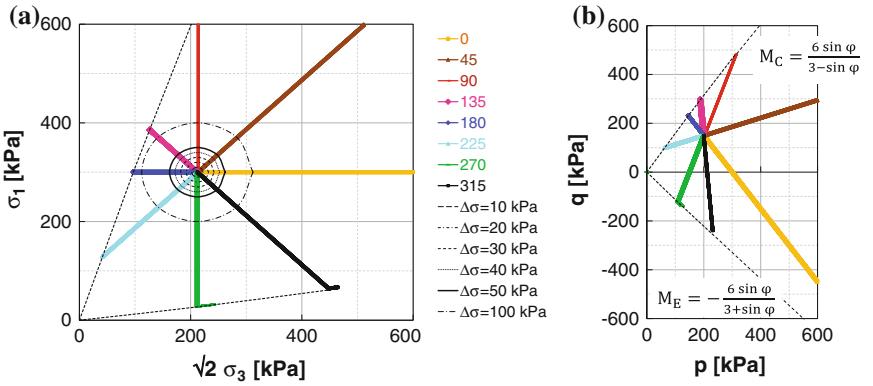

Fig. 13 Applying monotonous stress probes (here from stress-state A) in the rendulic-plane (**a**) and in the p-q-plane (**b**)

4 Experimental Results from Monotonous Loading

To obtain strain response-envelopes from monotonous loading paths, once a chosen initial stress-state is reached and consolidation is finished, a stress path in one direction is applied until failure, Fig. 13.

Total strains $\Delta\varepsilon$ are evaluated for different stress increments $\Delta\sigma = 20$, 30, 40, 50 and 100 kPa (circles in Fig. 13a).

Figure 14 shows different strain response-envelopes determined experimentally for 3 different stress-states located in compression (A), extension (J) and on the isotropic axis (I), which have the same mean pressure $p = 200$ kPa, but different stress-ratios η, Fig. 12.

From the stress-state located on the isotropic axis (I), the shape of the strain response-envelopes for $\Delta\sigma \leq 50$ kPa is almost similar to a symmetrical ellipse, Fig. 14b. For the 2 other stress-states (A and J), the strains due to stress probes indicating towards the failure-lines are significantly larger and the envelopes get elongated, Fig. 14a, c.

5 Experimental Results from Low Cycle Loading

5.1 Test Procedure to Determine Quasi-Elastic Strain-Response-Envelopes

To obtain quasi elastic strains for different stress probe directions, after consolidation at a chosen stress-state (Fig. 12), stress cycles of relatively small stress increments $\Delta\sigma \leq 50$ kPa are applied in a certain direction α_σ (Fig. 3). To avoid pore water pressure the frequency of the cycles was kept low.

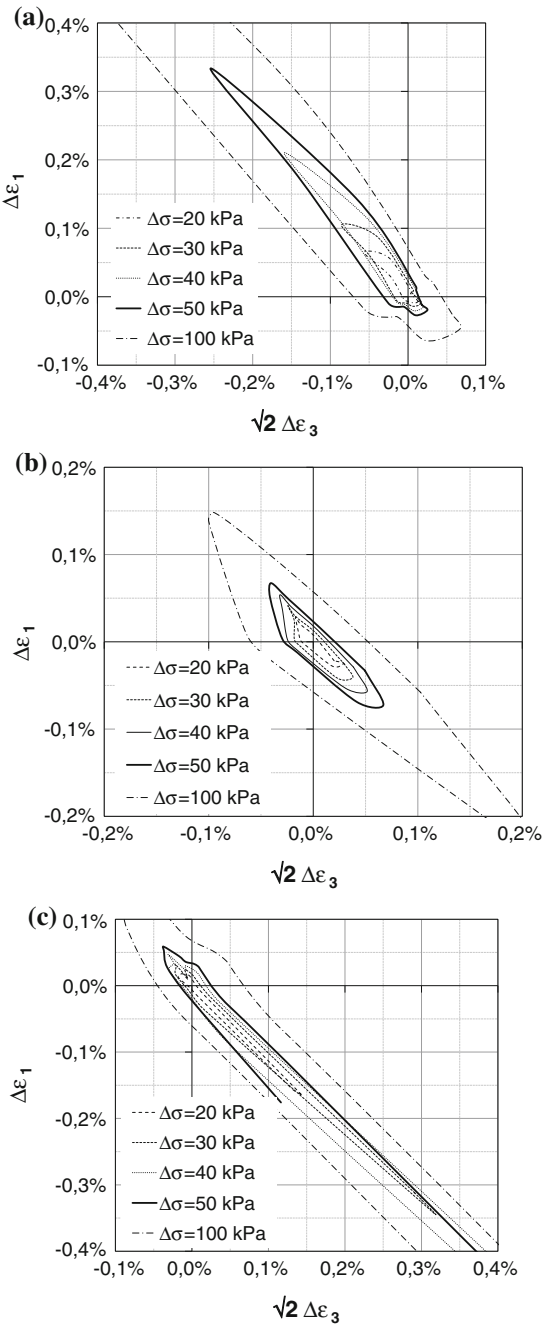

Fig. 14 Strain response-envelopes for stress-states A (**a**), I (**b**) and J (**c**) due to monotonous loading

The cyclic load in the first direction is repeated until the measured strains are practically reversible or rather quasi-elastic. The definition of "quasi-elasticity" implies that during one cycle the plastic strains are less than 1...3 % of the total strains, see Hettler and Danne [13]. It turns out that quasi-elastic behaviour can occur after a low number of cycles. The strain response of the last cycle of one direction is evaluated and plotted. After that, the test is continued by applying the same size of stress increment $\Delta\sigma$ in a different direction α_σ in the stress-space until quasi-elastic behaviour occurs again. The corresponding strains of the last cycle are plotted in a diagram, Fig. 15b.

The investigation of

1. the influence of the sequence of the directions,
2. the mean pressure p,
3. a monotonous isotropic prestress and
4. the stress-ratio η

on the shape, size and inclination of the response-envelope, i.e. the direction-dependent quasi-elastic stiffness, is described in the following.

5.2 Shape of the Quasi-Elastic Strain-Response-Envelopes

Figure 15 shows the quasi-elastic strain response-envelopes evaluated for different stress increments $\Delta\sigma$. In general, the envelopes seem to have the shape of symmetrical ellipses for different stress increments $\Delta\sigma$ and seem to be similar to each other, which may indicate a certain approximate linearity for investigated strain regime.

The highest absolute values of quasi-elastic strains always occur in the directions $\alpha_\sigma \approx 125° \ldots 135°$ and $\alpha_\sigma \approx 305° \ldots 315°$ (deviatoric un- and reloading with $\Delta p = 0$); the smallest absolute values result from directions $\alpha_\sigma \approx 35° \ldots 45°$ and $\alpha_\sigma \approx 215° \ldots 225°$(isotropic un- and reloading with $\Delta q = 0$).

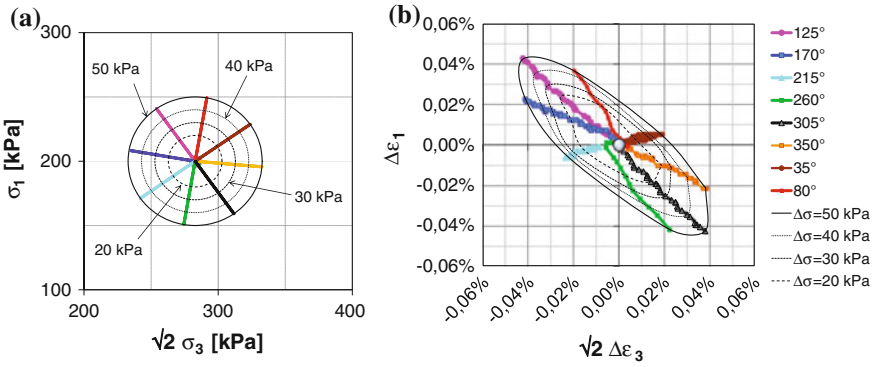

Fig. 15 Construction of the strain response envelope (here at stress-state I): **a** application of $\Delta\sigma =$ 50 kPa in 8 different directions and **b** corresponding strain-responses

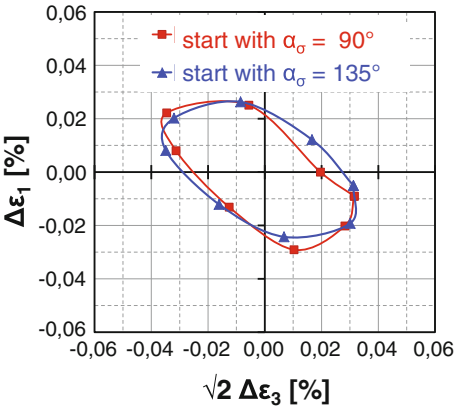

Fig. 16 Response-envelopes due to $\Delta\sigma = 50$ kPa for 2 different sequences of stress-paths from the same initial stress-state

5.3 Different Sequences of Stress Paths

To investigate the influence of the sequence of the applied stress-paths on the quasi-elastic strain-responses, the testing procedure described in Sect. 5.1 was applied for different sequences of directions α_σ. The rotational direction was also varied (clockwise and counter clockwise). It was found, that—for the investigated initial stress-states—neither the sequence nor the rotational direction of the applied stress-paths lead to a substantial influence on the strain response-envelopes, Fig. 16.

Further tests have been carried out which seem to confirm these results.

5.4 Stress-Dependent Stiffness

To investigate the stress-dependency of the quasi-elastic stiffness at low-cycle loading tests at 3 different initial stress-states with constant stress-ratios η and different mean pressures p are performed. The quasi-elastic strains due to stress increments $\Delta\sigma = 50$ kPa were determined and plotted by means of response-envelopes, Fig. 17.

As shown in Fig. 17b the size of the ellipses decreases with increasing mean pressure p and shows an increasing quasi-elastic stiffness for decreasing mean pressure p. This is especially evident at the stress-probe directions at deviatoric un- and reloading ($\alpha_\sigma = 125°$ and $\alpha_\sigma = 305°$). The influence of p on the elastic moduli at the directions $\alpha_\sigma = 35°$ and $\alpha_\sigma = 215°$ (isotropic un- and reloading) is much lower.

Figure 18 shows the absolute value of total strains $\Delta\varepsilon$ depending on the stress increment direction α_σ for 3 different stress-states at the same initial stress-ratio η = const. = 0.75.

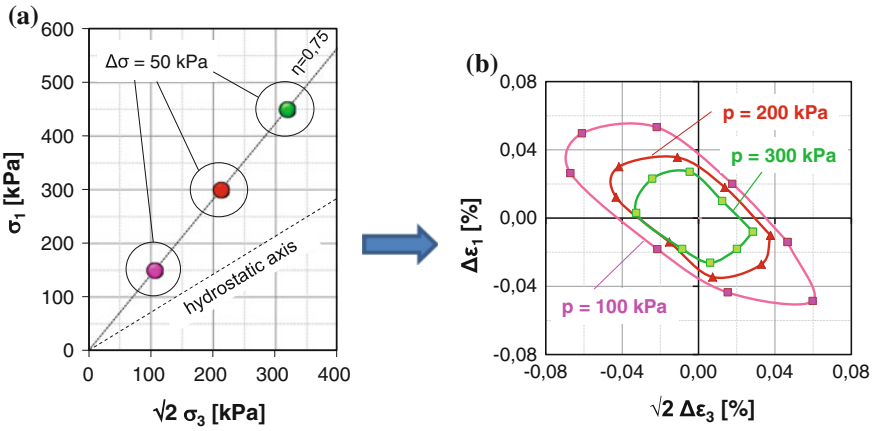

Fig. 17 Construction of the strain response envelope (here at stress-state I): **a** application of $\Delta\sigma$ = 50 kPa in 8 different directions and **b** corresponding strain-responses

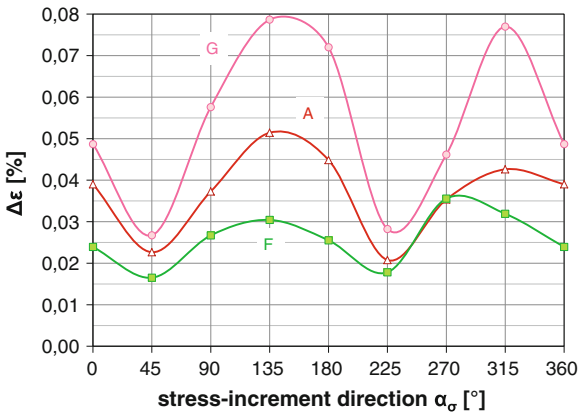

Fig. 18 Dependence of the absolute value of $\Delta\varepsilon$ on the stress increment direction α_σ (here for stress-states G, A and F with η = const. = 0.75)

5.5 *Isotropic Prestress*

To examine the influence of a static isotropic preloading on the size and shape of the quasi-elastic response-envelopes, different tests were carried out starting at the same initial stress state with and without preloading, Fig. 19.

It seems that the influence of an isotropic preloading is negligible, Fig. 20.

Similar observations were made when applying an anisotropic preloading. It will be also necessary to investigate the influence of stress histories in general ("histori-otropy") on quasi-elastic properties.

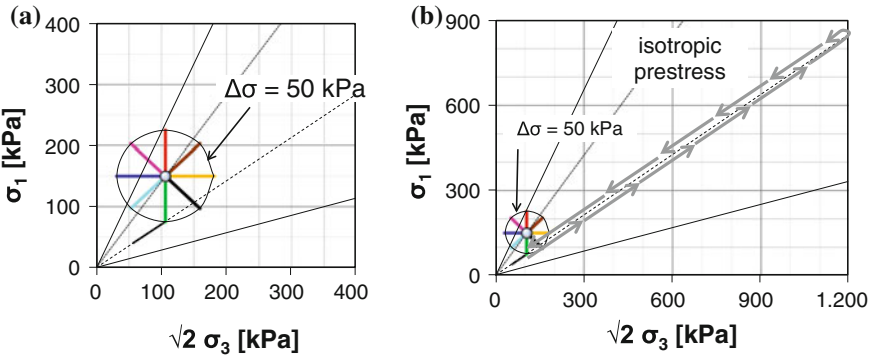

Fig. 19 Investigation of an isotropic prestress at stress-state G: experiment without (**a**) and with isotropic prestress (**b**)

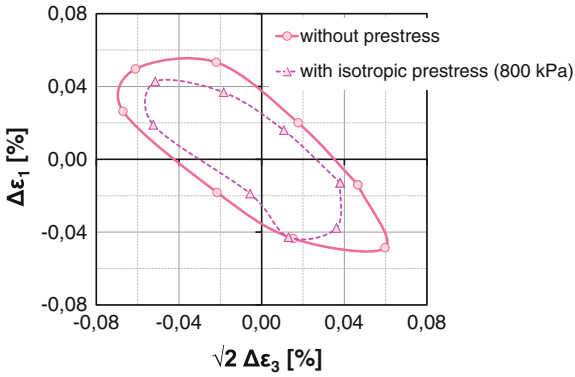

Fig. 20 Response-envelope due to $\Delta\sigma = 50$ kPa with and without prestress at stress-state G

5.6 Anisotropy

To investigate anisotropic material properties, tests were carried out for different initial stress-ratios η. Figure 21 shows the corresponding envelopes plotted in the p-q-plane.

A considerable rotation of the main axes of the response-envelopes depending on the initial stress ratio η can be observed. This influence can be quantified. Figure 22 shows the ratio E_v/E_h of the vertical quasi-elastic stiffness $E_v = \Delta\sigma_v/\Delta\varepsilon_v$ and the horizontal quasi-elastic stiffness $E_h = \Delta\sigma_h/\Delta\varepsilon_h$ as a function of the stress-ratio η. For this purpose data were analysed for stress-probes $\alpha_\sigma = 90°$ and 270° (axial compression and extension) and $\alpha_\sigma = 0°$ and 180° (radial compression and extension).

The dependence of the ratio E_v/E_h on the initial stress-ratio η can be interpreted as a **stress-induced anisotropy**. Similar observations are also made when investigating much smaller stress- or strain-cycles, e.g. Ezaoui and Di Benedetto [9] or Hoque and Tatsuoka [14]. The coarser the sand, the more distinctive is the difference between E_v

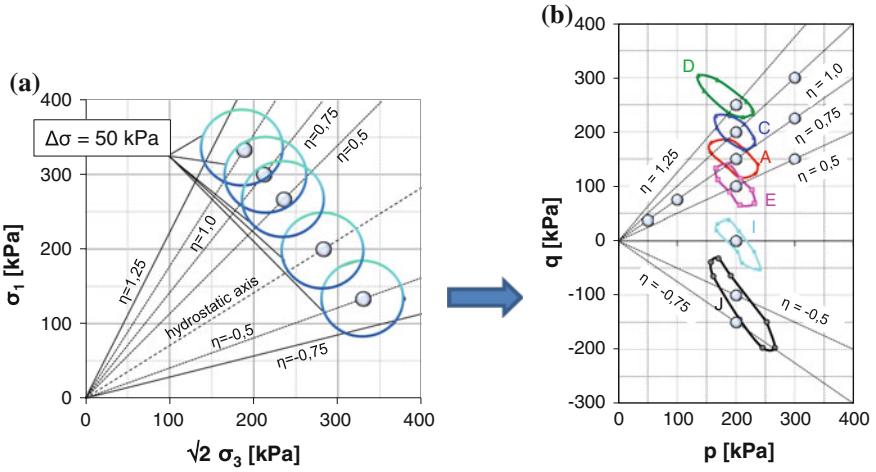

Fig. 21 Tests with different initial stress-ratios η and p = const. = 200 kPa: rotation of axes of the response-envelopes depending on the stress-ratio η

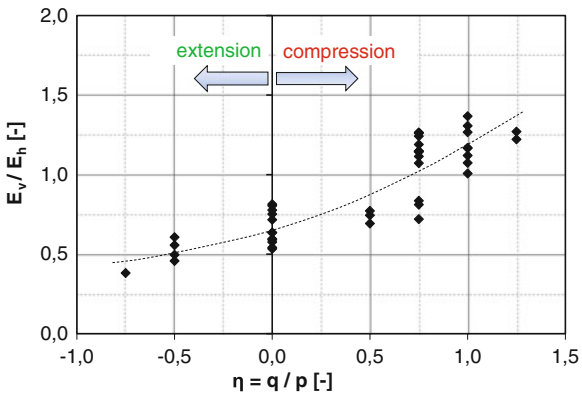

Fig. 22 Ratio of the quasi-elastic moduli E_v/E_h depending on the initial stress-ratio η

and E_h, i.e. the ratio E_v/E_h increases, Hoque and Tatsuoka [14]. A detailed analysis shows a stronger influence of the stress-ratio η on the vertical than on the horizontal stiffness, see Bellotti et al. [3].

Figure 22 does not only show a stress induced anisotropy. At the isotropic stress-state with $\eta = 0$ the ratio E_v/E_h is $\neq 1$. This means, that there are no isotropic properties at an initial isotropic stress-state, i.e. there also is an **inherent anisotropy**. Most authors come to similar conclusions. While Kuwano [16] and Hoque and Tatsuoka [14] find out $E_v/E_h \geq 1$ for all tested sands at isotropic stress-states, Ezaoui and Di Benedetto [9] also find ratios $E_v/E_h < 1$ for the preparation-methods pluviation and vibration and thus demonstrates a dependence of this ratio on the specimen preparation-method. These discrepancies seem to be due to several factors e.g. the grain-size distribution, the shape of the specimen and the preparation-method.

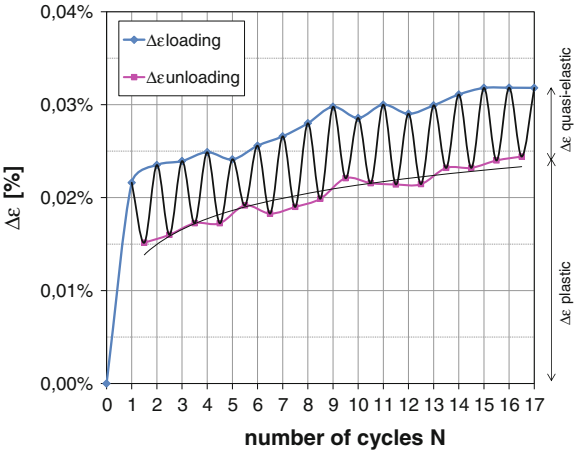

Fig. 23 Example of accumulation of strains $\Delta\varepsilon$ due to stress-probe-direction $\alpha_\sigma = 35°$ and $\Delta\sigma = 50$ kPa (initial stress-state I)

5.7 Plastic Strains

To investigate the accumulation of strains for small stress increments ($\Delta\sigma \leq 50$ kPa) one can look separately onto each stress probe direction, where stress cycles are performed. Figure 23 exemplarily shows the development of strains from loading and unloading with a stress-amplitude of $\Delta\sigma = \pm 25$ kPa in the direction $\alpha_\sigma = 35°$ (isotropic un- and reloading).

As expected, the strains increase with increasing number of cycles N. In Fig. 23 the accumulation of total strains becomes approximately 0 after about N = 15 cycles. Considering the pure quasi-elastic strains, i.e. the difference between $\Delta\varepsilon_{\text{loading}}$-$\Delta\varepsilon_{\text{unloading}}$, it seems that there is hardly any change of the absolute value of the quasi-elastic strains with the number of cycles N. For the construction of the strain response-envelopes shown in the previous sections, this means that the size of the quasi-elastic envelopes remains approximately constant and is independent of the number of stress-cycles.

6 Summary and Further Hints

Producing experimental or numerical response-envelopes is a convenient tool to investigate the soil's incremental stress-strain behaviour and to compare, calibrate or validate constitutive equations.

Most available experimental data are typically obtained by testing a soil in few loading conditions. In this paper an attempt is made to evaluate the incremental stress-strain behaviour for several loading directions, starting from many different initial stress-states.

From monotonous loading paths it could be shown, that from the stress-state located on the isotropic axis, the shapes of the strain response envelopes for

$\Delta\sigma \leq 50$ kPa are almost similar to symmetrical ellipses. For other stress-states the strains due to stress probes indicating towards the failure-lines, are significantly larger and the envelopes get elongated in this direction.

The investigation of the incremental stress-strain behaviour of sand at low-cycle loading in triaxial testing shows, that for investigated stress-increments $\Delta\sigma \leq 50$ kPa quasi-elastic behaviour can occur after a low number of cycles. While the influence of the sequence of the stress-paths as well as isotropic preloading on the quasi-elastic strains seems to be negligible, a significant influence of the mean pressure p and the initial stress-state η on the size and the inclination of the strain-response-envelopes can be observed.

Further triaxial tests are necessary in order to investigate e.g. the influence of the void ratio, K_0-preloading and the stress history in general (historiotropy). It may also be relevant to find out whether there is an influence of the direction of sedimentation during pluviating the sand sample on the anisotropic properties.

It is known, that some common constitutive models show deficits when predicting deformations due to high and low-cycle loading processes, e.g. ratcheting in hypoplasticity, elastic behaviour after the first un- and reloading in elastoplastic constitutive models, missing anisotropy. It is intended to use the presented results together with future tests as a basis for calibrating and validating more complex constitutive equations especially developed for low-cycle loading processes [8, 19].

Acknowledgments The work presented in this paper was supported by the German Research Foundation (DFG) as subproject 8 "Incremental stress-strain-behaviour of sand at low-cycle loading and application on excavation-models" of the interdisciplinary research group FOR 1136 "Simulation of geotechnical construction processes with holistic consideration of the stress strain soil behaviour (GeoTech) "Incremental stress-strain behaviour". The authors appreciate the financial support from the DFG.

References

1. Anandarajah, A., Sobhan, K., Kuganenthira, N.: Incremental stress-strain behaviour of granular soil. J. Geotech. Eng-ASCE **1**, 57–68 (1995)
2. Baldi, G., Nova, R.: Membrane penetrations effect on triaxial testing. J. Geotech. Eng-ASCE **110**(3), 403–420 (1984)
3. Bellotti, R., Jamiolkowski, M., Lo Presti, D.C.F., O'Neill, D.A.: Anisotropy of small strain stiffness in Ticino sand. Géothechnique **46**(1), 115–131 (1996)
4. Calvetti, F., Viggiani, G., Tamagnini, C.: A numerical investigation of the incremental behaviour of granular soils. R.I.G. 11–19 (2003)
5. Costanzo, D., Viggiani, G., Tamagnini, C.: Directional response of a reconstituted fine-grained soil—Part I: experimental investigation. Int. J. Numer. Anal. Meth. **13**, 1283–1301 (2006)
6. Danne, S., Hettler, A.: Verhalten von nichtbindigen Böden bei niederzyklischer Belastung. Geotechnik **36**, 19–29 (2013)
7. Doanh, T.: Strain response envelope: a complementary tool for evaluating hostun sand in triaxial compression and extension: experimental observations. In: Constitutive Modelling of Granular Materials, pp. 375–396. Springer, Berlin (2000)
8. Ehlers, W., Avci, O.: Stress-dependent hardening and failure-surfaces of dry sand. Int. J. Numer. Anal. Meth. 1–23 (2011)

9. Ezaoui, A., Di Benedetto, H.: Experimental measurements of the global anisotropic elastic behaviour of dry hostun sand during triaxial tests, and effect of sample preparation. Géothechnique **59**(7), 621–635 (2009)
10. Goldscheider, M.: Shakedown and incremental collapse of structures in dry sand bodies. In: Proceedings of Dynamical Methods in Soil and Rock, Plastic and Long-Term Effects in Soils (1977)
11. Gudehus, G.: A comparison of some constitutive laws for soils under radially symmetric loading and unloading. In: Balkema, Proceedings of the 3rd International Conference on Numerical Methods in Geomechanics, pp. 1309–1323. W. Wittke (2001)
12. Hettler, A.: Verschiebungen starrer und elastischer Gründungskörper in Sand bei monotoner und zyklischer Belastung. Heft 90, Veröffentlichungen des Instituts für Bodenmechanik und Felsmechanik der Universität Fridericiana in Karlsruhe (1981)
13. Hettler, A., Danne, S.: Strain response-envelopes for low-cycle loading processes. In: Proceedings of the 18th International Conference on Soil Mechanics and Geotechnical Engineering, pp. 1491–1494. Paris (2013)
14. Hoque, E., Tatsuoka, F.: Anisotropy in elastic deformation of granular materials. Soils Found. **38**(1), 163–179 (1998)
15. Kolymbas, D.: Response-envelopes: a useful tool aus "Hypoplasticity then and now". In: Kolymbas, D., (ed.) Constitutive Modelling of Granular Materials, pp. 57–105. Springer, Berlin (2000)
16. Kuwano, R., Jardine, R.J.: On the application of cross-anisotropic elasticity to granular materials at very small strains. Géothechnique **52**(10), 727–749 (2002)
17. Lewin, P.I., Burland, J.B.: Stress-probe experiments on saturated normally consolidated clay. Géothechnique **20**(1), 38–56 (1970)
18. Nicholson, P.G., Seed, R.B., Anwar, H.A.: Elimination of membrane compliance in undrained triaxial testing. I. Measurement and evaluation. Can. Geotech. J. **30**, 727–738 (1993)
19. Niemunis, A., Prada-Sarmiento, L., Grandas-Tavera, C.: Paraelasticity. Acta Geotech. **6**(2), 147, 67–80 (2011)
20. Niemunis, A., Wichtmann, T., Triantafyllidis, T.: A high-cycle accumulation model for sand. Comput. Geotech. **32**(4), 245–263 (2005)
21. Royis, P., Doanh, T.: Theoretical analysis of strain response-envelopes using incrementally non-linear constitutive equations. Int. J. Numer. Anal. Meth. **22**, 97–132 (1998)
22. Sibille, L.: Directional stress probes to exhibit constitutive behaviour of discrete element models. Olek Zienkiewicz Course 2011—Discrete Mechanics of Geo-materials, Grenoble, June 27th-July 1st (2011)
23. Tamagnini, C., Masýn, D., Costanzo, D., Viggiani, G.: An evaluation of different constitutive models to predict the directional response of a reconstituted fine-grained soil. In: Modern Trends in Geomechanics, pp. 143–157. Springer, Berlin (2006)